Pure & Appl. Chem., Vol. 67, No. 6, pp. 931–938, 1995.
Printed in Great Britain.

Solid electrolytes

John B. Goodenough

Center for Materials Science & Engineering, ETC 9.102, The University of Texas at Austin, Austin, Texas 78712-6019, U.S.A.

Abstract: The application of solid electrolytes in electrochemical cells is used as a basis for establishing quality criteria for these materials. Emphasis is given to the electrolyte window and the bulk ionic conductivity in the design of a solid electrolyte. Fast ionic conduction in stoichiometric compounds is characterized by a transition from long-range to short-range ordering that may be smooth or first-order. Smooth transitions involving cluster excitations are contrasted with first-order transitions involving ionic ordering within an array of otherwise equivalent lattice sites or a displacive transition of the fixed-ion array. Ionic conduction in doped compounds is hindered by trapping at the dopants as well as by interactions between the mobile species that introduce short-range ordering. Water absorption may plague oxide-ion electrolytes. Illustrative examples are cited.

BACKGROUND

Quality Criteria

An electrolyte is an ionic conductor and an electronic insulator. Ideally it conducts only one ionic species, a condition that is more easily satisfied in a solid than in a liquid. Electrolytes find their primary application in electrochemical cells. Solid electrolytes are particularly useful where the reactants of the electrochemical cell are either gaseous or liquid.

Electrochemical cells are of two types: power cells and sensors. In an ideal power cell, the ionic current through the electrolyte inside the cell matches an electronic current through an external load. A solid electrolyte acts as a separator of the two electrodes as well as a carrier of the internal ionic current. It is in the form of a membrane of thickness L and area A that separates electronically the two electrodes of the cell. Any internal electronic current across the electrolyte reduces the power output. The internal resistance to the ionic current is

$$R_i = L/\sigma_i A \qquad (1)$$

where σ_i is the ionic conductivity of the electrolyte. For a current I through the cell, the voltage IR_i represents a potential drop that is to be minimized. Even in potentiometric sensors, the resistance R_i must be maintained below a certain level to obtain satisfactory sensitivity and speed of response, and any electronic contribution to the internal cell current must be factored into the cell calibration.

These simple considerations lead to the following general quality criteria for a solid-electrolyte material to be used in an electrochemical cell.

1. To minimize R_i for a given intrinsic σ_i, the material must lend itself to easy fabrication into a mechanically strong membrane of small L and large A. Optimization of cell design may also require the fabrication of membranes of complex shape.

2. Unless an exceptionally small L/A ratio is feasible, an acceptable R_i generally requires a $\sigma_i > 10^{-2}$ Scm^{-1} at the cell operating temperature T_{op}. Note: In general, the conductivity is a tensor, but for polycrystalline electrolytes a scalar σ_i is used.

3. A transport number

$$t_i \equiv \sigma_i/\sigma \approx 1 \text{ where } \sigma = \Sigma_j \sigma_j + \sigma_e \qquad (2)$$

is needed. In general, there is only one mobile ion in a solid electrolyte so that $\Sigma_j \sigma_j = \sigma_i$. Because any electronic mobility is much greater than the ionic mobility, only a relatively small number of electronic carriers can make the electronic conductivity σ_e competitive with σ_i, *i.e.* $\sigma_e \geq \sigma_i$, to degrade t_i to an unacceptable level.

4. The resistance to ion transfer across the reactant/electrolyte interface must also be low.

5. Chemical stability in the working environment requires that the electrolyte is neither reduced by the reductant at the negative electrode nor oxidized by the oxidant at the positive electrode. Thermodynamic stability is only achieved by placing the bottom of the solid-electrolyte conduction band above the highest

occupied molecular orbital (HOMO) of the reductant and the top of the solid-electrolyte valence band below the lowest unoccupied molecular orbital (LUMO) of the oxidant as illustrated in Fig. 1. Note: Where the reactants are the metallic electrodes, as in a storage battery, the energies of the HOMO and/or LUMO are given by the Fermi energy of the anode and/or cathode.

6. The mobile ion of a solid electrolyte must be the working ion of the cell.
7. The cost of material and fabrication is always a consideration.

Given these quality criteria, the challenge is to design a material that meets all these demands at a useful operating temperature T_{op}. In order to meet this challenge, it is necessary first to understand the factors that limit and control these quality criteria. In this paper, only the conduction mechanisms that control σ_i for an anionic electrolyte are addressed. However, attention is called to the need for a large energy gap E_g between the valence and conduction bands of the electrolyte and an absence of localized states within this gap if a $t_i \approx 1$ is to be ensured; and the edges of the valence and conduction bands must be matched to the operating environment to ensure chemical stability.

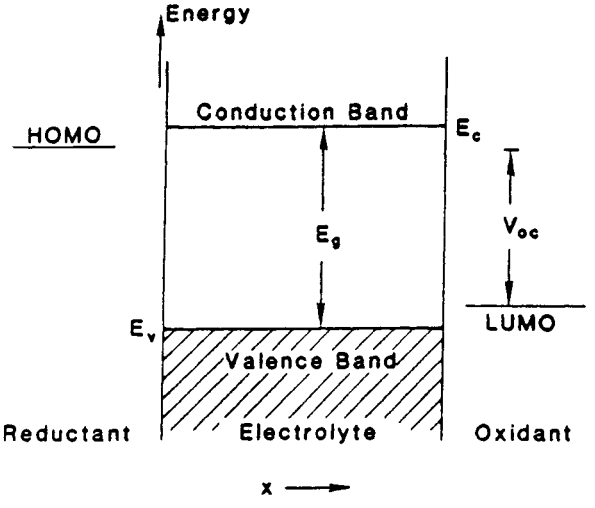

Fig. 1 Placement of reactant energies relative to the edges of the electrolyte conduction and valence bands in a thermodynamically stable electrochemical cell at flat-band potential.

Ionic Conductivity: Phenomenology

In a polycrystalline membrane, the scalar expression for the mobile-ion current density has the form

$$\mathbf{i}_D = \sigma_i \mathbf{E} = c_i q \mathbf{v} \tag{3}$$

where $\mathbf{v}$ is the mean velocity of the mobile ions of charge q and concentration c_i. From the definition of the charge-carrier mobility $u = \mathbf{v}/\mathbf{E}$, we have the scalar ionic conductivity

$$\sigma_i = c_i q u \tag{4}$$

Since long-range ionic motion in a solid is diffusive, we have from the Nernst-Einstein relation

$$u = qD/kT \tag{5}$$

where the diffusion coefficient

$$D = D_o \exp(-\Delta G_m/kT) \tag{6}$$

contains the motional free energy $\Delta G_m = \Delta H_m - T\Delta S_m$. Substitution of (5) and (6) into (4) gives

$$\sigma_i = (A_D/T)\exp(-E_a/kT) \tag{7}$$

where, for a mobile-ion site occupancy $n_c = c_i/C$ on an array of energetically equivalent sites of concentration C,

$$E_a = \Delta H_m \tag{8}$$

$$A_D = (Cq^2/k)n_c D_o \exp(\Delta S_m/k) \tag{9}$$

To obtain a more complete description, we need to find an analytic expression for D_o. From the theory of random walk, which neglects correlated motions of the ions, a

$$D_o \approx (l^2/6)z(1-n_c)f\nu_o \tag{10}$$

is derived; $\nu_o \approx 10^{12}s^{-1}$ is the jump-attempt frequency and l is the distance an ion jumps to reach one of the z near-neighbor equivalent sites that is empty with a probability $(1-n_c)$. The factor f is introduced to allow a correction for the neglected correlation between ionic movements. Substitution of (10) into (9) gives

$$A_D = \gamma(Cq^2/k)n_c(1-n_c)l^2\nu_o \tag{11}$$

$$\gamma = f(z/6)\exp(\Delta S_m/k) \tag{12}$$

If n_c is not temperature-independent, but varies as

$$n_c = n_o \exp(-\Delta H_i/2kT) \tag{13}$$

then n_c in (11) is replaced by n_o and (8) becomes

$$E_a = \Delta H_m + (\Delta H_i/2) \quad (14)$$

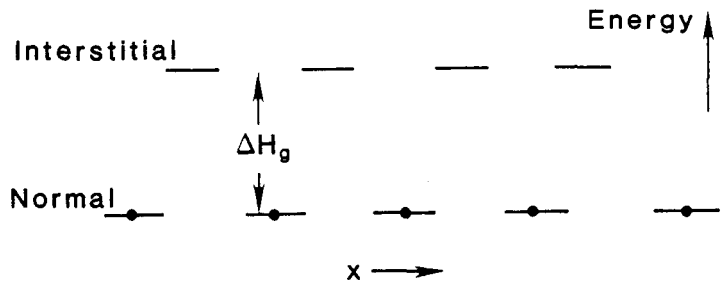

Fig. 2 Energies of a working ion in a stoichiometric ionic compound: the dots indicate an occupied site.

Stoichiometric Compounds

At low temperatures, stoichiometric ionic solids have arrays of crystallographically equivalent sites completely filled with ions. We designate these sites as *normal* in order to distinguish them from *interstitial* sites having a higher ionic potential energy. The highest normal-site ionic energies are separated from the lowest interstitial-site energies by an energy gap ΔH_g as illustrated in Fig. 2; this ionic gap is analogous to the electronic energy gap E_g of an electronic insulator. No ionic conduction is possible on the normal sites if they are all filled, and there are no mobile ions in the interstitial sites if they are all empty. In most ionic solids, ΔH_g is not strongly temperature-dependent below the sintering temperature, and any ionic conduction requires near-sintering temperatures to excite ions from normal to interstitial positions, *i.e.* to make Frenkel defects so as to create arrays of equivalent sites that are only partially occupied.

On the other hand, there are some stoichiometric ionic solids that undergo an order-disorder transition for only one ionic species at a transition temperature T_t that is below the melting point T_m. Where the order-disorder transition for one ionic species leaves the other atoms in their original positions, as occurs in PbF_2 and LaF_3, this phenomenon has been referred to as *sublattice melting* (1). These transitions may be smooth or first-order. Where the order-disorder transition induces a structural transformation of the other ions, as occurs in AgI where disordering of the Ag^+ ions induces a transformation of the iodide-ion array from close-packed to body-centered cubic, the transition is first-order at T_t. In either case, the energy gap ΔH_g for the mobile-ion species becomes strongly temperature-dependent as T approaches T_t, vanishing for $T > T_t$. An order parameter for the transition, which may be either smooth or first-order as illustrated in Fig. 3, is the ratio $\Delta H_g(T)/\Delta H_g(0)$ of the gap at temperature T relative to its value of T = 0 K. At temperatures $T > T_t$, a set of energetically equivalent sites of concentration C is partially occupied, and the site occupancy $n_c = c_i/C$ of mobile ions would be a constant independent of temperature were there no short-range order. In fact, the probability that an ion can jump to a neighboring site with only a motional enthalpy ΔH_m is reduced by a lowering of $(1 - n_c)$ due to the short-

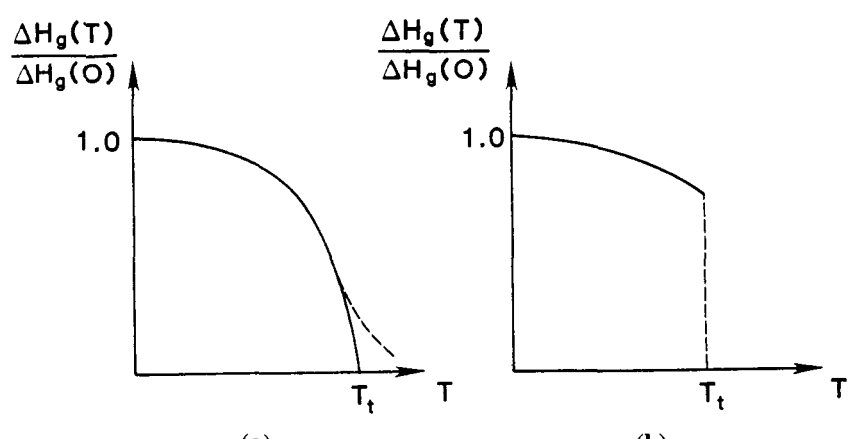

Fig. 3 The order parameter $\Delta H_g(T)/\Delta H_g(0)$ for an order-disorder transition that is (a) smooth, (b) first-order

range order; this lowering introduces a temperature-dependent contribution to E_a that is to be added to the temperature-independent motional enthalpy ΔH_m. At temperatures $T < T_t$, the site occupancy $n_c = c_i/C \sim \exp(-\Delta H_g/2kT)$ varies according to the law of mass action in a manner analogous to the concentration of electrons and holes in an intrinsic semiconductor. However, in this case ΔH_g is not temperature-independent;

$$\Delta H_g(T) = \Delta H_g(0) - n_c\varepsilon \tag{15}$$

since ΔH_g decreases as the amount of thermally induced disorder increases. It is the positive feedback through the temperature dependence of n_c that makes possible a first-order order-disorder transition at T_t.

In addition to $\Delta H_g(T)$, the total activation energy

$$E_a = \Delta H_m + (\Delta H_g/2) \quad \text{for } T < T_t \tag{16}$$

contains a motional enthalpy ΔH_m. This thermal energy needed for a jump contains two components, a barrier energy ΔH_b for the ion to hop when the acceptor and donor sites are at the same energy and a relaxation energy ΔH_r that must be supplied to make energetically equal the acceptor and donor sites:

$$\Delta H_m = \Delta H_b + \Delta H_r \tag{17}$$

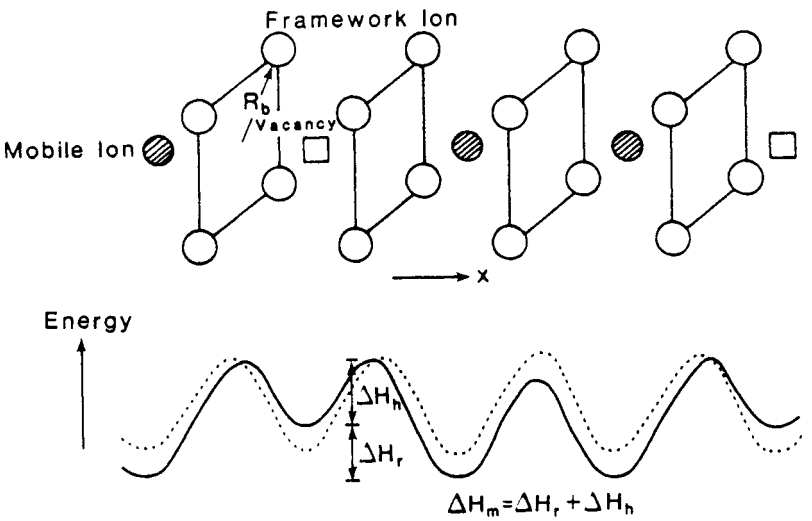

Fig. 4 Definition of "bottleneck" shortest distance R_b and variation of mobile-ion potential with position with (solid line) and without (dotted line) relaxation of the host structure.

If the sites on which a mobile ion moves share common faces, as illustrated in Fig. 3, or common edges, the site face or edge acts as a barrier to the ionic motion. In order for an ion to pass through a common face, for example, the shortest distance R_b from the center of the face to a peripheral ion must be large enough to allow it to pass. Where R_b is smaller than the sum of the radii of the mobile and a peripheral ion, thermal energy must be supplied to open up the interface; where R_b is larger than the sum of the ionic radii, thermal energy may need to be supplied to push the mobile ion into the center of the diffusion pathway. Even where R_b is roughly equal to the sum of the ionic radii, thermal energy must be supplied to the mobile ion to push it over the maximum in the potential energy curve at the saddle-point position. In Equation (17), ΔH_b is minimized by matching the mobile-ion size to R_b. The relaxation energy ΔH_r is present because the time it takes for an ion to hop over the barrier ΔH_b is long compared to the time it takes the immobile ions to relax to their equilibrium positions, which are different at the empty and occupied sites. To minimize ΔH_r, it is necessary to match the mobile-ion size to the volume of the site it occupies. These two constraints are incompatible with one another, and the lowest values of ΔH_m are found where the effective sum of the ionic radii can be modified by a polarization (or quadripolarization) of the peripheral and/or the mobile ions. In AgI, for example, the large I^- ions are readily polarized and the Ag^+ ion can hybridize its $4d^{10}$ core with empty 5s states so as to change the shape of its repulsive core from a sphere to a prolate ellipsoid; the hybridization energies involved in the polarization of the I^- ion and the quadripolarization of the Ag^+ ion are largely compensated by the gain in the covalent component of the Ag-I bond. Such an

accommodation of the Ag-I bond length permits the size constraints of both ΔH_r and ΔH_b to be nearly optimized simultaneously to give a low $\Delta H_m \approx 0.05$eV.

Non-stoichiometric Compounds

Where there is no order-disorder transition temperature $T_t < T_m$ above which ΔH_g collapses or where T_t is much higher than the desired operating temperature T_{op} of the electrolyte, it is customary to employ doping strategies to create mobile-ion vacancies or interstitials as charge compensation. In the stabilized zirconia $Zr_{1-x}Ca_xO_{2-x}$, for example, the substitution of Ca^{2+} for Zr^{4+} not only stabilizes the fluorite structure; it also introduces oxygen vacancies to compensate for the smaller charge on the Ca^{2+} ion. Superficially, the creation of oxygen vacancies is analogous to the introduction of holes into the valence band of silicon by doping with boron. However, the diffusive motion of ions as against the itinerant character of the valence-band electrons in silicon quite changes the magnitude of the energy ΔH_t by which a mobile ionic species is trapped at the dopant that creates it. In the ionic case

$$\Delta H_t = \Delta H_c + \Delta H_r \tag{18}$$

contains, in addition to the coulombic term ΔH_c, a relaxation term ΔH_r due to the diffusive character of the motion. Also, the term ΔH_c is larger because the ionic charges are less effectively screened by the dielectric constant of the solid. It is not unusual to find a $\Delta H_t > 1$ eV, which makes

$$E_a = \Delta H_m + 0.5\Delta H_t \tag{19}$$

disappointingly large. In $Zr_{1-x}Ca_xO_{2-x}$, for example, the larger Ca^{2+} ion relative to Zr^{4+} creates a local elastic strain field that adds to the coulombic attraction of the oxygen vacancies to a Ca^{2+} ion, and an $E_a \geq 1$ eV makes $T_{op} > 800$°C. In order for the oxygen vacancy to contribute to a d.c. conductivity, it must either free itself from the dopant or find a tortuous percolation pathway through the solid. However, doping heavily enough to provide the percolation pathways and operation at a high T_{op} tends to make the material metastable with respect to a clustering of the dopants and deeper trapping of the oxygen vacancies. Aging is a problem in the stabilized zirconias where relatively heavy doping is required to stabilize the fluorite structure.

EXAMPLES

Stoichiometric compounds

The compounds PbF_2, $Ba_2In_2O_5$, and AgI illustrate fast ionic conduction in stoichiometric compounds. Like stabilized zirconia, PbF_2 has the fluorite structure; but as a stoichiometric compound the F^- ions occupy all the tetrahedral sites of the face-centered-cubic Pb^{2+} ion array. Nevertheless Faraday first noted a smooth transition to fast F^--ion conduction in this compound at higher temperatures. $Ba_2In_2O_5$ is a fast oxide-ion conductor above a first-order order-disorder transition at $T_t \approx 930$°C that leaves the BaIn array unchanged. AgI is a fast Ag^+-ion conductor above a first-order transition at a $T_t = 147$°C; in this case the stationary I^--ion array changes from close-packed to body-centered cubic at T_t.

In the case of PbF_2, a fundamental problem has been the characterization of the disordered state at high temperatures. It was reasonable to anticipate that the F^- ions were being excited from the tetrahedral sites of the Pb^{2+}-ion array, the normal sites, into interstitial octahedral sites. However, Schultz (2) has analyzed high-temperature x-ray-diffraction data with asymmetric F^--ion potentials to show that the F^- ions are not thermally excited to the octahedral sites, but spend an increasing percentage of their time at the saddle-point positions between tetrahedral sites as the temperature is raised. In order to understand this rather surprising result, it is instructive to consider the room-temperature structure of KY_3F_{10} shown in Fig.

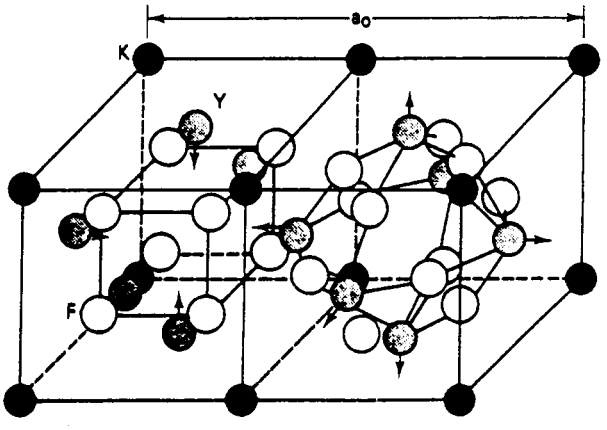

Fig. 5 Two quadrants of the cubic Ky_3F_{10} structure.

5. In this structure, the K^+ and Y^{3+} ions are ordered within a face-centered-cubic cation array as are the Au and Cu atoms in the alloy $AuCu_3$. The F^- ions are not evenly distributed within the interstitial space of this cation array, but are segregated into F^--poor quadrants containing F^- ions on all the tetrahedral sites as in the fluorite structure and F^--rich quadrants containing twelve F^- ions on all the saddle-point positions between the tetrahedral sites. This structure demonstrates two interesting points: first, there is little difference in the potential energy for F^- ions on tetrahedral and saddle-point positions in a face-centered-cubic cation array in confirmation of the x-ray studies of Schultz on PbF_2; second, the occupancy of saddle-point positions in one quadrant can coexist stably with the occupancy of tetrahedral sites in the neighboring quadrants. This latter observation demonstrates that in the fluorite structure of PbF_2 *cluster excitations* of eight F^- ions within a quadrant from tetrahedral sites to saddle-point positions are energetically accessible (3). This cooperative excitation is more accessible in PbF_2 than in isostructural SrF_2 because of the polarizability of the Pb^{2+}:$6s^2$ core, which reduces ΔH_m. The energetic accessibility of a cluster excitation to saddle-point sites of larger concentration allows a disordering of the F^- ions over tetrahedral and saddle-point sites, which in turn permits long-range F^--ion diffusion with a relatively small $E_a = \Delta H_m + 0.5\Delta Hg(T)$. Ionic transport requires local charge fluctuations that stabilize a greater occupancy of saddle-point sites at the expense of F^--ion vacancies introduced into neighboring fluorite quadrants. In this case, the temperature dependence of $\Delta Hg(T)$ is weak, so the order-disorder transition is smooth. The thermodynamic consequences of such a model have not been studied either theoretically or experimentally.

The structure of the ideal cubic ABO_3 perovskite has an ordered AB cation array consisting of two interpenetrating simple-cubic A and B cation arrays. The oxygen atoms occupy the midpoints of the edges of the cube of smaller B cations to give an array of corner-shared BO_6 octahedra. At room temperature, $Ba_2In_2O_5$ has the brownmillerite structure of Fig. 6(a) (4); it is an oxygen-deficient perovskite $BaInO_{2.5}$ with an ordering of the oxygen vacancies within alternate In-O planes perpendicular to an orthorhombic *c*-axis. An In^{3+} ion is stable in either octahedral or tetrahedral coordination, and the vacancy ordering creates corner-shared planes of InO_6 octahedra sharing corners along the *c*-axis with corner-shared planes of InO_4 tetrahedra. Ordering of the anion vacancies makes the vacancy and occupied oxygen sites crystallographically and energetically inequivalent; the energy of the vacancy sites is separated from that of the occupied sites by an energy gap $\Delta Hg(T) = \Delta Hg(0) - n_c\varepsilon$, Equation (15). In this case, a strong positive feedback into $\Delta Hg(T)$ through the temperature dependence of n_c induces a first-order order-disorder transition at $T_t = 930°C$ (5) as shown in Fig. 6(b). The slope of $\log(\sigma T)$ *vs.* $1/T$ well above T_t gives a measure of ΔH_m; but just above T_t considerable short-range order persists (6). Below room temperature, the slope of $\log(\sigma T)$ *vs.* $1/T$ gives a measure of $E_a = \Delta H_m + 0.5\Delta H_g(0)$. As T approaches T_t, a $d\Delta H_g(T)/dT < 0$ introduces an anomalous increase with temperature in the magnitude of the slope of the $\log(\sigma T)$ *vs.* $1/T$ plot as well as an anomalous increase in the pre-exponential factor A_D.

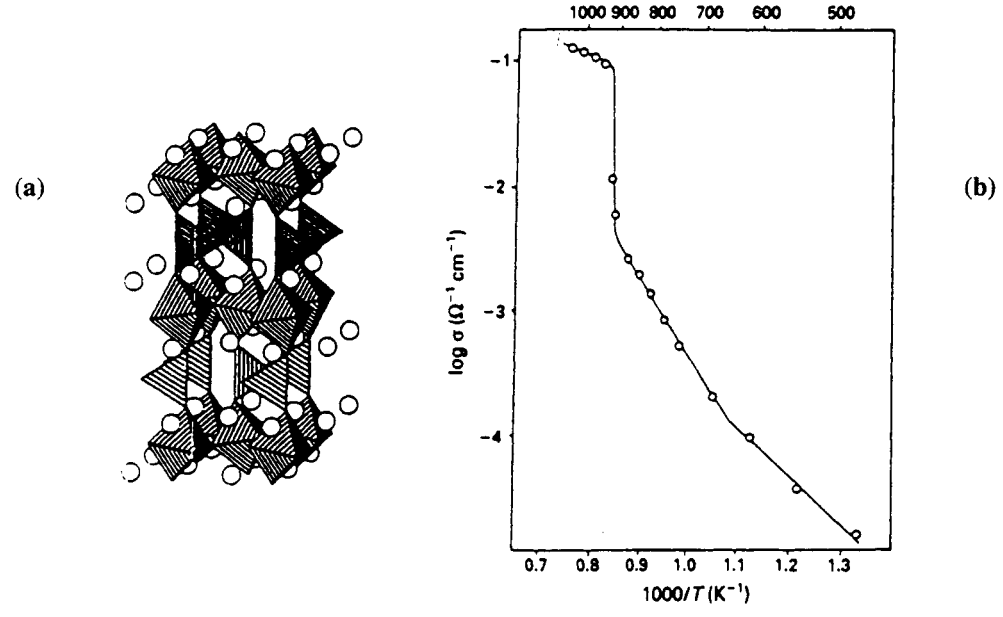

Fig. 6 $Ba_2In_2O_5$: (a) brownmillerite structure $T < T_t$ and (b) conductivity *vs.* reciprocal temperature.

A similar, but somewhat different situation is present in AgI. In this case, the Ag^+ ions are ordered on half the tetrahedral sites of a close-packed I^--ion array at low temperatures. Thermal excitation of Ag^+ ions into interstitial sites induces at T_t = 147°C a first-order displacive transition of the I^- sublattice from close-packed to body-centered cubic with Ag^+ ions partially occupying equivalent face-sharing pseudotetrahedral sites (7). Although only one of the four tetrahedral sites in a cube face can be occupied simultaneously, there are three cube faces for two Ag^+ ions, so the Ag^+ ions only occupy two-thirds of the available tetrahedral sites, which gives an $E_a = \Delta H_m \approx 0.05$ eV. Partial substitution of Rb for Ag led to the compound $RbAg_4I_5$ having a rigid RbI_5 array within which the Ag^+ ions are disordered at room temperature over an array of face-shared tetrahedral sites (8). Although the $E_a = \Delta H_m$ is a little higher in $RbAg_4I_5$ than in high-temperature AgI, nevertheless stabilization of fast ionic conduction to room temperature was a major achievement. A key to retention of a small ΔH_m in $RbAg_4I_5$ is the ordering of the Rb^+ ions into a fixed position in this compound.

Non-stoichiometric electrolyte

The number of stoichiometric compounds exhibiting technically useful ionic order-disorder transitions is extremely limited, and no practical strategy exists for identifying where to look for them. Consequently most attempts at the design of solid electrolytes have relied on chemical doping. In this approach, the mobile species are trapped by an energy ΔH_t at the dopant that creates them to give an $E_a = \Delta H_m + 0.5\Delta H_t$, Equation (19). The materials design problem is then to find a way to reduce ΔH_m and ΔH_t simultaneously.

The development of framework (or skeleton) structures has proven an excellent strategy for alkali-ion solid electrolytes (9). In this approach, doping within the framework is sufficiently removed from the mobile-ion species that ΔH_t is minimized; and an open framework can provide an interstitial space that minimizes ΔH_m. Presumably a similar strategy could be developed for anion conductors. However, to date work has concentrated on substitutions into fixed cation arrays within which the anions are mobile. Simple cation arrays allow three-dimensional conduction; layered structures confine the anion conduction to two dimensions within alternate layers. Attempts to develop a good oxide-ion electrolyte illustrate the problems encountered with this approach to obtain anion conductors.

Oxide-ion Electrolytes

The stabilized zirconias continue to be the oxide-ion electrolyte of choice; but these have an $E_a \approx 1$ eV, which forces a $T_{op} > 800$°C. It is a high ΔH_t that is responsible for the high value of E_a. In $Zr_{1-x}Ca_xO_{2-x}$, for example, the oxygen vacancies make direct contact with the substituted cation array, and they tend to be trapped at Ca^{2+} ions as discussed above. Moreover, stabilization of the fluorite structure requires the introduction of enough vacancies that vacancy-vacancy interactions tend to stabilize regions of short-range order that, in turn, may induce Ca^{2+}-ion clustering at a high T_{op}. This situation provides a strong motivation to search for alternate oxide-ion electrolytes.

The ordered AB cation array of the cubic ABO_3 perovskite structure offers an alternate cation array, and the experiments in $Ba_2In_2O_5$, Fig. 6, demonstrate that ΔH_m can be acceptably small in this cation array if the vacancies are disordered. To disorder the vacancies, it is necessary to reduce their concentration. Ideally that would be done by going to cation substitutions that leave an ordered cation array. In fact, another tack was taken.

The compound $Ca_3Fe_2TiO_8$ is reported (10) to have an anion-deficient perovskite structure in which the oxygen vacancies order so as to give a plane of corner-shared BO_4 tetrahedra alternating with two planes of corner-shared BO_6 octahedra, *i.e.* ...OOTOOT... *vs.* the ...OTOT... stacking of Fig. 6(a); the Fe and Ti B cations remain disordered. Because the Zr^{4+} ion is unstable in less than sixfold oxygen coordination, it was reasoned that the Zr^{4+} ions would tend to capture six oxygen near neighbors to leave the oxygen vacancies associated with the In^{3+} ions. Competition for capturing oxygen at Zr^{4+} ions in the BO planes would create vacancies in the BO_2 planes so as to promote disorder and oxygen conduction (5). In fact, a fast ionic conduction was observed below 400°C, but it turned out to be protonic associated with H_2O absorbed below 400°C into the oxygen vacancies (11). Under dry conditions, oxygen is absorbed, oxidizing the oxide-ion array. Two important conclusions follow:

1. Where an ABO_{3-y} cubic perovskite contains B cations stable in tetrahedral as well as octahedral sites, there is little driving force to absorb neutral oxygen species so as to transform BO_4 tetrahedra to BO_6 octahedra.
2. Where the B cations are unstable in less than sixfold oxygen coordination, oxygen and/or water absorption occurs in oxygen-deficient perovskites to complete the sixfold oxygen coordination.

Ions like Zr^{4+}, Hf^{4+}, Ce^{4+}, Y^{3+}, or Ln^{3+} are unstable in less than sixfold oxygen coordination; they prefer eightfold oxygen coordination. Stabilized zirconia does not absorb water because the Zr^{4+} ion

always has at least sevenfold oxygen coordination in the fluorite structure. On the other hand, ions like Al^{3+}, Ga^{3+}, and In^{3+} are stable in either fourfold or sixfold coordination; these ions form the brownmillerites $A_2B_2O_5$ and do not absorb water at low temperatures. These ions should, therefore, be used in oxide-ion electrolytes based on the oxygen-deficient perovskite structure.

This conclusion has been reinforced by two studies. In the first, substitution of Y^{3+} for In^{3+} in $Ba_2In_2O_5$ yielded $Ba_3Y_4O_9$, a phase stable in dry air. In moist air, $Ba_3Y_4O_9$ decomposes into Y_2O_3 and $BaCO_3$. A fast ionic conduction observed in the range $370 < T < 600°C$ for a starting pellet of $Ba_3Y_4O_9$ turned out to be protonic; it occurs in an immobilized-liquid state of an intermediate decomposition product $Ba(OH)_2$-BaO_{2-x} and/or a eutectic $Ba(OH)_2$ - 11 w/o $BaCO_3$ (12). In the second study, $LaGaO_3$ was doped by substitution of Sr^{2+} for La^{3+} and/or Mg^{2+} for Ga^{3+} so as to introduce a controlled concentration of oxygen vacancies (13,14). The system $La_{2-x}Sr_xGa_{1-y}Mg_yO_{3-0.5z}$, $z = x + y$, does not absorb water or oxygen from moist air, it does not age at 750°C, and it has an oxide-ion conductivity about 3 times higher than stabilized zirconia above 550°C. However, a measured $E_a = 1.07$ eV below 600°C is somewhat larger than the 0.98 eV activation energy obtained in the best yttria-stabilized zirconia. Clearly ΔH_t remains a problem in this point-doped oxide. What makes it a superior electrolyte is a pre-exponential factor A_D that is about 20 times larger than that of yttria-stabilized zirconia. An unusually large value for A_D signals either a large entropic term $\exp(\Delta S_m/k)$ or the addition of a factor associated with a temperature-dependent component in E_a. This situation is found on the approach to an order-disorder transition, which suggests a smooth order-disorder transition, associated with short-range ordering of the oxygen vacancies is taking place below 600°C.

An interesting variation of this approach is found in the O^{2-}-ion conductors $Bi_4V_{2-x}M_xO_{11-y}$ first studied by Abraham *et al* (15). $Bi_4V_2O_{11}$ itself is a layered compound containing oxygen vacancies. A fixed Bi_2O_2 layer alternates with an oxygen-deficient $VO_{5.5}$ layer to give two-dimensional oxide-ion conduction; but high oxide-ion conductivities are only found above a smooth order-disorder transition temperature $T_t \approx 570°C$. Substitution of 20% of the V^{5+} ions, and also some Bi^{3+} ions (16), by the Jahn-Teller ions Cu^{2+} or Mn^{3+} and/or by the ferroelectric Ti^{4+} or Nb^{5+} ions suppresses the cooperative distortions of the lower-temperature phases and gives a remarkably high O^{2-}-ion conductivity above 200°C. Although the transport number t_O is reported to be high in air at temperatures $T > 500°C$, the presence of transition-metal cations and of Bi^{3+} ions makes too restrictive for many applications the range of partial pressures over which t_O is high. Nevertheless, the use of ions active in displacive transitions to enhance the ionic conductivity is instructive.

Proton Electrolytes

Finally, the ability of the proton to make directed hydrogen bonds makes difficult the design of proton conductors useful at higher temperatures. Fast proton conduction within an oxide only occurs where thermal energies excite the OH^-, H_2O, and/or H_3O^+ species into free rotation. However, this situation is found in solids only on the approach to loss of water. The best solid proton conductors are wet particle hydrates (17,18), which restricts their use to near ambient temperatures.

REFERENCES

1. M. O'Keeffe and B.G. Hyde, *Phil. Mag.* **33**, 219 (1976).
2. H. Schultz, *Prog. 2nd European Conf. Solid State Chem.* Veldhoven, Netherlands, eds. R. Metselaar, H.J.M. Heijligers, and J. Schoonman, Elsevier, Amsterdam, (1982) p. 117.
3. J.B. Goodenough, *Proc. Roy. Soc. (London)*, **A393**, 215 (1984).
4. K. Mader and H.K. Müller-Buschbaum, *J. Less Common Metals*, **157**, 71 (1990).
5. J.B. Goodenough, J.E. Ruiz-Diaz, and Y.S. Zhou, *Solid State Ionics*, **44**, 21 (1990).
6. T.R.S. Prasanna and Alexandra Navrotsky, *J. Mater. Res.* **8**, 1484 (1993).
7. L.W. Strock, *Z. Phys. Chem.* **B25**, 441 (1934); A.F. Wright and B.E.F. Fender, *J. Phys. C* **10**, 2261 (1977).
8. J.N. Bradley and P.D. Greene, *Trans Faraday Soc.* **62**, 2069 (1966); B.B. Owens and G.R. Argue, *Science* **B157**, 308 (1967).
9. J.B. Goodenough, H.Y-P. Hong, and J.A. Kafalas, *Mat. Res. Bull* **11**, 203 (1976).
10. J. Rodriguez-Carvajal, M. Vallet-Regi, and J.M. Gonzalez-Calbet, *Mat. Res. Bull.* **24**, 423 (1989).
11. A. Manthiram, J.-F. Kuo, and J.B. Goodenough, *Solid State Ionics* **62**, 225 (1993).
12. Man Feng and J.B. Goodenough, *Solid State Ionics* **68**, 269 (1994).
13. T. Ishihara, H. Matsuda, and Y. Takita, *J. Am. Chem. Soc.* ***116****, 3801 (1994).*
14. Man Feng and J.B. Goodenough, *European J. Solid State Inorg. Chem.* (in press).
15. F. Abraham, M.F. Debreville-Gresse, G. Mairesse, and G. Nowogrocki, *Solid State Ionics* **28-30**, 529 (1988); **40-41**, 934 (1990).
16. C.K. Lee, G.S. Lim, and A.R. West, *J. Mater. Chem.* (in press).
17. W.A. England, M.G. Cross, A. Hamnett, P.J. Wiseman, and J.B. Goodenough, *Solid State Ionics* **1**, 213 (1980).
18. J.B. Goodenough, *Methods in Enzymology* **127**, 263 (1986).